Available online at www.sciencedirect.com
SCIENCE DIRECT®
PERGAMON
Solid State Communications 126 (2003) 373–378
solid state communications
www.elsevier.com/locate/ssc

Thermoelectric power, magnetoresistance of lead chalcogenides in the region of phase transitions under pressure

Vladimir V. Shchennikov, Sergey V. Ovsyannikov*

Institute of Metal Physics, Urals Division of Russian Academy of Sciences, High Pressure Group, 18 S. Kovalevskaya Str., 620219 Yekaterinburg, GSP- 170, Russian Federation

Received 9 December 2002; received in revised form 6 March 2003; accepted 12 March 2003 by L.V. Keldysh

Abstract

The longitudinal and transverse thermomagnetic Nernst–Ettingshausen (N–E) effects were measured at ultrahigh pressure up to 20 GPa under closure of semiconductor gap at NaCl- and GeS-type phases of n-PbTe, p-PbSe and p-PbS. Near ~3 GPa, the maxima of N–E effects and magnetoresistance (and hence of mobility of charge carriers) attributed to gapless state for PbTe and PbSe were established. The reversible sign inversion of transverse N–E effect indicating the change in scattering mechanism of charge carries have been revealed at high pressure phase of PbSe. The lowering of thermomagnetic effects with pressure gave the evidence of indirect semiconductor gap at high pressure GeS-type phases in contrary to NaCl-phases.

PACS: 72.15.Gd; 72.20.Nz; 62.50 + p

Keywords: A. Semiconductors; D. Electronic transport; D. Galvanomagnetic effects; D. Phase transitions; E. High pressure

1. Introduction

The investigations of kinetic effects at high pressure P are known to be an effective method for study of electron structure of semiconductors [1,2]. The behaviour of kinetic coefficients under pressure (decreasing or increasing, the rate of changing) allows to check the theoretical predictions and, thus, to chose correct physical model of electron structure [1,2]. Till recently the list of kinetic effects available under ultrahigh pressure included electrical resistance [3], thermoelectric power S [4], and magnetoresistance (MR) measurements [5]. The investigations of thermomagnetic (TM) effects depending crucially on the scattering mechanism of charge carriers and the type of electron structure (direct or indirect energy gap) were available only at small range of hydrostatic pressures 0–3 GPa [6,7]. By using synthetic diamond anvils, the technique of TM measurements have been developed up to 30 GPa [8], and the investigations of transverse (TNE) and longitudinal (LNE) Nernst–Ettingshausen (N–E) effects have been performed at elemental semiconductors with one-band type of conductivity Te and Se near semiconductor–metal phase transitions [8]. But it was a question of applicability of the above TM technique for investigations of micro-samples of more complex semiconductors, where electrons and holes give a contribution to conductivity.

In present paper, IV–VI Group narrow gap semiconductors PbX (X — Te, Se, S) were taken for investigations by the TM technique at high pressure. At ambient conditions, PbTe, PbSe and PbS have direct semiconductor gap $E_g \approx$ 0.29, 0.27, 0.41 eV, respectively, at L point of Brillouin zone [9] lowering under pressure ($dE_g/dP \approx -0.08$ eV/GPa) [9]. Above ~2.5, ~4.5 and ~5.2 GPa, they transform into GeS-type lattice [9–13] and at 12–21 GPa — to CsCl-type structure [12] with metal conductivity [14,15]. At GeS-lattice, PbTe, PbSe and PbS are n-type semiconductors with estimated values of $E_g \sim$ 0.1, 0.4 and 0.6 eV decreasing under pressure until semiconductor–metal transition [15]. So, E_g twice gradually closes at PbX under pressure in

* Corresponding author. Tel.: +7-3432-783545; fax: +7-3432-745244.
E-mail address: vladimir.v@imp.uran.ru (V.V. Shchennikov).

0038-1098/03/$ - see front matter © 2003 Elsevier Science Ltd. All rights reserved.
doi:10.1016/S0038-1098(03)00210-2

NaCl- and GeS-phases. The purpose of present work was to measure TM N–E effect at high pressure of up to 20 GPa in investigating the mobility μ and effective mass m of charge carriers both at initial and high pressure phases of PbX at the closure of semiconductor gap. Till now TM effects at PbX were measured only at ambient pressure [6,9].

2. Experimental technique

The technique of TM measurements under pressure is described in Ref. [8]. Synthetic diamond anvils as well as tungsten carbide ones were used for pressure generation in solid medium of catlinite; the values of pressure P were estimated with an error ± 10% from calibration curves [4,8]. Three diamond chambers with working diameters from 0.6 to 1.0 mm were used (Fig. 1).

Diamond anvils served as a heater and a cooler for creation of thermal gradient ΔT along a sample [4,8,16,17]. The values of thermal difference were estimated by measurements of temperature at fixed points of the anvils [8,16]. Values of S were determined from linear dependence of thermoelectric voltage on thermal gradient ΔT (insert on Fig. 2). Measurements were carried out both in stationary and non-stationary thermal regime [8,17] to exclude the influence of the heater electric current.

In diamond anvils the samples were disk-shaped about ~0.05–0.02 thickness and ~0.3 mm in diameter. Sizes of samples in tungsten carbide chamber ~$0.4 \times 0.4 \times 0.2$ mm^3. Well conducting diamond anvils and also thin Pt–Ag ribbons of 5 μm thickness were used as electrical leads to samples [4,8,15]; the corrections were made for S values taking into account, the contributions from anvils [4,8,15–17].

At fixed pressures S- and MR- measurements were carried out under stationary magnetic field B up to 2 T produced by electro-magnet (Fig. 1). Due to asymmetric location of electrical leads at semiconductor samples the contribution of even and odd on B effects (Hall effect into MR, etc.) usually persists [18,19]. This circumstance was used in our experiments for the measurement of longitudinal and transverse N–E effects by turning of chamber around its axis (Fig. 1) [8]. An automated setup was used allowing one to record and store in the memory the several parameters of environment (B, ΔT, etc.) and electrical signals from a sample [8,17]. For investigation, the single crystals of n-PbTe, p-PbSe and p-PbS were taken with concentrations of electrons (holes) at room temperature: 1.5×10^{18}, 1.1×10^{18} and 1×10^{18} cm^{-3}, respectively.

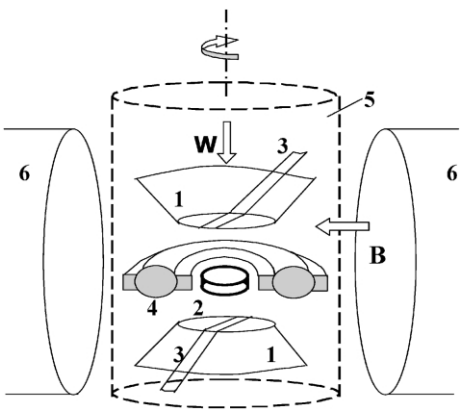

Fig. 1. Experimental high pressure setup: **1** — diamond anvils; **2** — sample; **3** — potential probes to sample (platinum–silver ribbons); **4** — catlinit gasket; **5** — high pressure chamber, **6** — electro-magnet. Arrows show the direction of magnetic field B and thermal flow W generating thermal gradient along a sample.

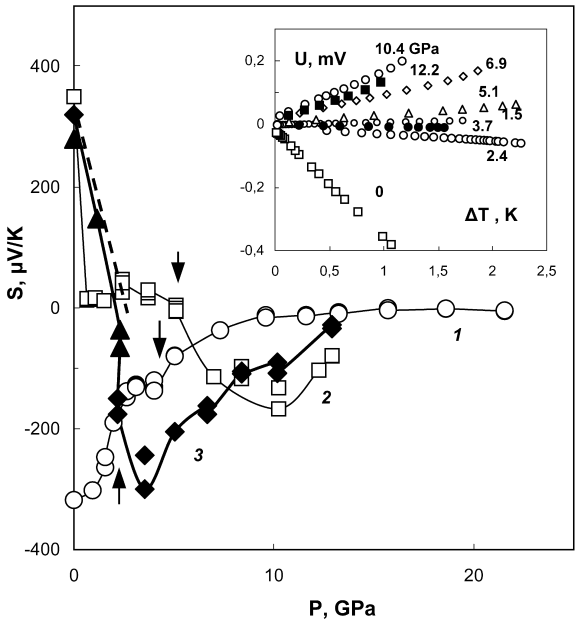

Fig. 2. Dependencies of thermoelectric power S on pressure P for n-PbTe (**1**), p-PbSe (**2**) and p-PbS (**3**) at 295 K. For p-PbS, the data obtained at tungsten carbide (black triangles) and diamond (black rhombuses) anvils. Dashed lines represent theoretical dependece of $S(P)$ for PbSe and PbS in one-band approximation: $dS/dP = (1/2eT)\, dE_g/dP$ (see text). The arrows show the beginning of structural transformation [9,12] to GeS-type lattice. At the insert there are dependencies of thermoelectric voltage U on temperature gradient ΔT along a sample for p-PbSe at 295 K and different pressures (shown at the plot).

3. Experimental results and discussion

Electrical resistance (not shown) and S of p-PbS, p-PbSe and n-PbTe crystals decreased under P both in NaCl- [20,21] and GeS-type phases; at phase transition these entities arose due to the opening of E_g (Fig. 2) [15]. The smoothing of S-jumps at phase transition in Fig. 2 is connected with quasihydrostatic pressure. However, the ethanol–methanol liquid mixture at $P \sim 1.5$ GPa, lower than P_t of structural transformation in PbTe, the Raman spectra of GeS-phase

were observed; the last were kept even at pressures ~5 GPa higher than P_t of transition into CsCl-lattice [13]. For non-degenerate semiconductor, the value of S is proportional to E_g : $S \approx (k/e)[(\sigma_n - \sigma_p)/(\sigma_n + \sigma_p)](E_g/2kT)$, where ρ the electrical resistivity, k the Boltzmann's constant, e the electron charge and σ_n and σ_p the electron and hole partial conductivities [18,19]. The decreasing of $S(P)$ for p-PbSe at NaCl-phase not only connected with dE_g/dP, but also with the increasing of σ_n (Fig. 2).

In Fig. 3, the typical dependencies of S on B are shown at different turns of chamber with a sample in magnetic field (Fig. 1). $S(B)$ signal consisted of linear and quadratic on B parts attributed to TNE and LNE effects, respectively [6,8, 18,19]. Coefficients Q of TNE effects were determined from linear part of $S(B)$ (Figs. 3–5). LNE effect was observed at turning of chamber with a sample through 90°; the rest linear on B part being deducted from the full $S(B)$ signal (Figs. 3–5).

S of p-PbS and p-PbSe samples changed its sign under P (Fig. 2) Variation of type of charge carriers may be accounted by the equations for MR and TNE effects for two-band model in weak magnetic fields ($\mu B < 1$) [6,9,19]:

$$\frac{\Delta\rho}{\rho} = B^2 b_r \times\left[\left(\frac{\sigma_n}{\sigma}\mu_n^2 + \frac{\sigma_p}{\sigma}\mu_p^2\right) - \left(\frac{\sigma_n}{\sigma}\mu_n - \frac{\sigma_p}{\sigma}\mu_p\right)^2 \frac{a_r^2}{b_r}\right] \quad (1)$$

$$Q = \frac{k_0}{e} a_r \times\left[r\left(\frac{\sigma_n}{\sigma}\mu_n + \frac{\sigma_p}{\sigma}\mu_p\right) + \frac{\sigma_n\sigma_p}{\sigma^2}(\mu_n + \mu_p)\left(2r + 5 + \frac{E_g}{kT}\right)\right] \quad (2)$$

where μ_n and μ_p the mobilities of electrons and holes, a_r and b_r are the constants, depending on scattering parameter r defining the dependence of relaxation time τ on electron energy ϵ : $\tau(\epsilon) \sim \epsilon^r$. At σ_n or $\sigma_p \to 0$ Eqs. (1) and (2) go to one-band case used for the analysis of experimental data. The sign of Q is determined by the sign of r only (in contrary to its galvanomagnetic analogue — Hall effect), as both electrons and holes are moving in the same direction under the temperature gradient action [6,18,19]. Contrary to TNE and MR, LNE effect (variation of S in transverse magnetic field), depends on the sign of charge carriers:

$$\Delta S_{II} = \frac{k_0}{e}(\mu B)^2 A_2 \quad (3)$$

For two-band conductivity one ought to replace the constant A_2 by the function depending on r, μ_n/μ_p, σ_n/σ_p and E_g [18]. In two opposite cases of acoustic phonons scattering ($r = -1/2$) and charged centres scattering ($r = 3/2$) the constant A_2 equals $A_2 \approx 9\pi/16(1 - \pi/8)$ and $A_2 \approx -30$, respectively, so, value of S increases (at $r = -1/2$) or

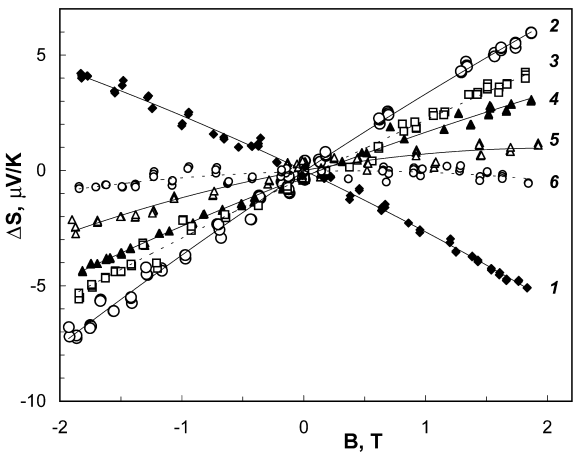

Fig. 3. Variation of thermoelectric power S on magnetic field B at consequent turns of high pressure chamber with p-PbSe sample at $T = 295$ K and $P = 2.4$ GPa. (**1**) — transverse Nernst–Ettingshausen effect, (**2**) — transverse N–E effect of opposite sign (after turn trough 180°), (**3**), (**4**), (**5**) — transient states between transverse and longitudinal N–E effects, (**6**) — longitudinal N–E effect (rotation through 90° from position **2**).

decreases (at $r = 3/2$) at magnetic field [18,19]. In experiments, the electrical voltages: $\Delta U_{\parallel}(B) = \Delta S_{\parallel}(B)\Delta T$ and $\Delta U \perp (B) = BQ\Delta T/(\Delta y/\Delta x)$ were measured, where Δx and Δy are the thickness and the distance between the electrical probes in Hall direction [8], respectively. Thus, TNE effect is proportional to both Q, and to ratio $\Delta y/\Delta x(\Delta y/\Delta x \sim 1)$.

The value of S having small positive value for p-PbSe (Fig. 2) decreased in magnetic field (Figs. 3 and 4). But the mobility of electrons in PbSe is essentially higher than one of the holes [9]. As most mobile charge carriers mainly contribute to quadratic on B effects [19] one may suppose that LNE effect in PbSe was just due to the electrons (Fig. 2). Then positive LNE effect (Fig. 4b) corresponded to the value of scattering parameter $r = -1/2$. Above 5 GPa (at GeS-phase) the inversion of sign of TNE effect occurred (Fig. 4a). The sign of LNE effect was also inverted (not shown). It corresponded to the inversion of r sign from negative $r = -1/2$ to positive one; so the dominant became the scattering by charged carriers ($r = 3/2$) or by optical phonons ($r = 1$) [18,19]. Above 8 GPa, both of the N–E effects became negligible. After the releasing of P, the reverse inversion of r sign was observed (Fig. 4)

Absolute value of S for n-PbTe increased in magnetic field B (Fig. 5), that also supposed the acoustic phonons scattering mechanism ($r = -1/2$) which is in agreement with the results of TM measurements at ambient conditions [6,9]. The increasing of both TM effects and MR for PbTe and PbSe under P were observed at NaCl-phase and decreasing of them were observed above $P > 3$ GPa (Figs. 3–5). For PbS there were no appreciable effects of S and ρ

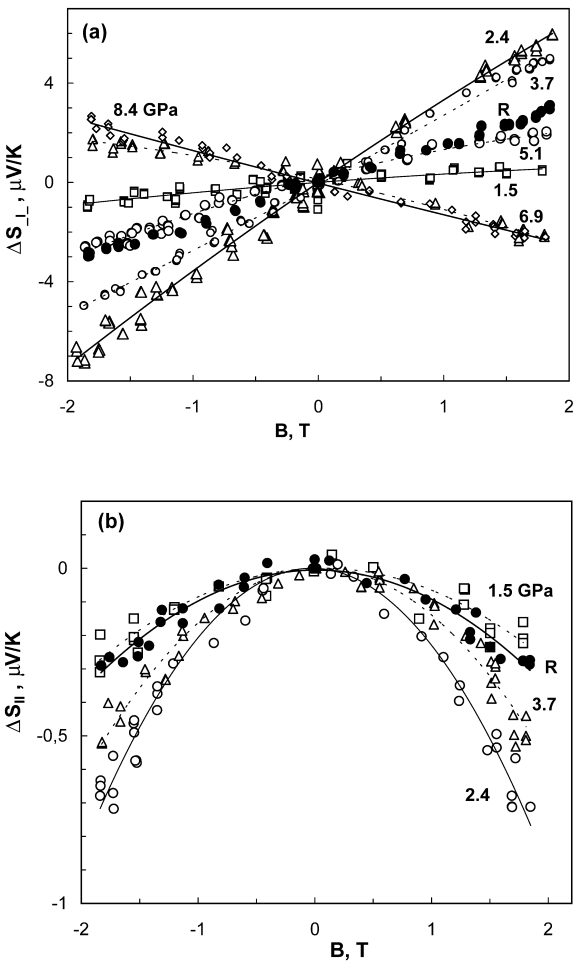

Fig. 4. Variation of transverse (a) and longitudinal (b) N–E effects on magnetic field B for p-PbSe at $T = 295$ K and fixed pressures (shown on the plot). Black circles marked by R have been obtained under pressure releasing (at ~2 GPa).

on B, for two samples both in diamond and in tungsten carbide chambers. This regularity agreed with the relation of μ at room temperatures: $\mu(\mathrm{PbS}) < \mu(\mathrm{PbSe}) < \mu(\mathrm{PbTe})$ [9].

According to Eqs. (1)–(3), the behaviour of MR and N–E effects reflected the variation of m and μ under pressure (Tables 1 and 2). The maxima of above effects and of μ near ~3 GPa (Tables 1 and 2) obviously corresponded to the transition of PbX into gapless state, where values of mobility $\mu \sim 1/m \sim 1/E_g$ ought to be the largest [9,18,19,22,23]. Values of μ obtained for PbSe and PbTe (Tables 1 and 2) accorded with typical ones at ambient pressure [6,9]. In a case of two-band conductivity the values of μ corresponded to 'effective' mobility, accounting contributions from different bands (for example, for semimetals $\mu = (\mu_n\mu_p)^{1/2}$ [19]). The lowering of N–E and MR effects under closure of $E_g(P)$ [15] at GeS-type phase (Figs. 4 and 5) indicated that E_g

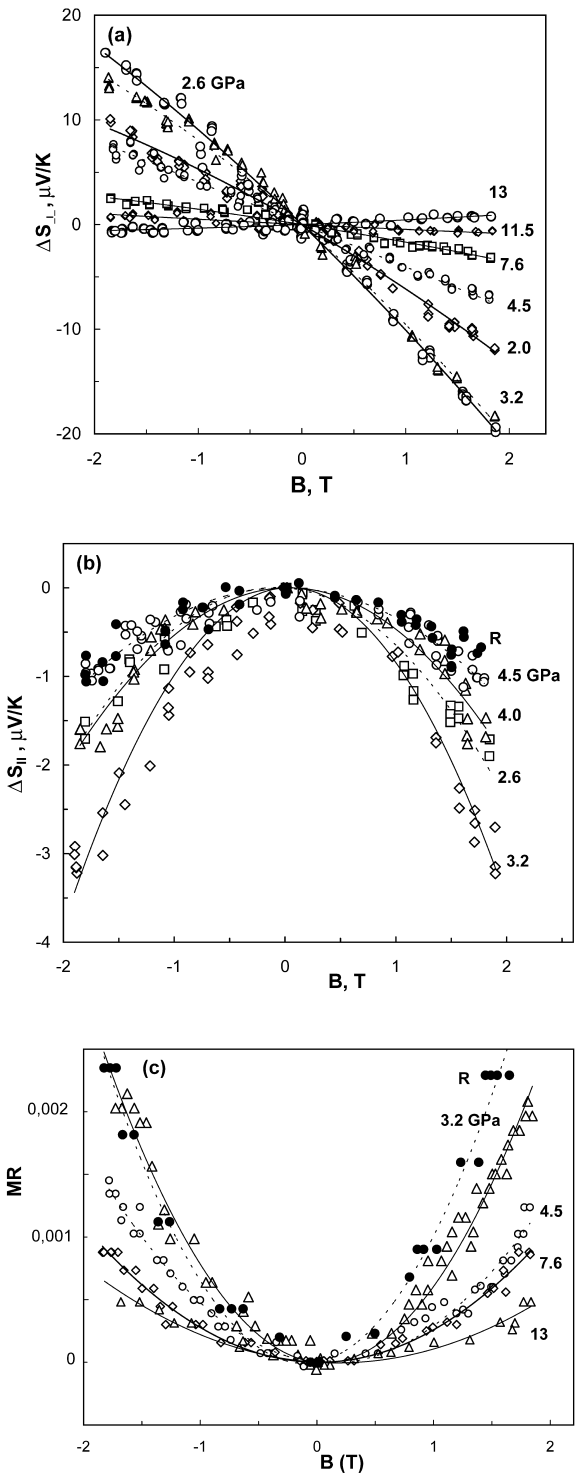

Fig. 5. Variation of transverse (a) and longitudinal (b) N–E effects and MR (c) on magnetic field B for n-PbTe at $T = 295$ K and fixed pressures (shown on the plot). Black circles marked by R have been obtained under pressure releasing (at ~3.2 GPa).

Table 1
Approximate values of charge carriers mobility for n-PbTe sample, estimated from transverse ($\mu_{TNE}(\Delta y/\Delta x)$) and longitudinal ($\mu_{LNE}$) Nernst–Ettingshausen effects and magnetoresistance (μ_{MR}) at $T = 295$ K

P (GPa)	μ (m^2/V s)		
	$\mu_{TNE}(\Delta y/\Delta x)$	μ_{LNE}	μ_{MR}
0	0.025	–	–
1.0	0.051	–	–
1.6	0.109	0.076	–
2.0	0.113	–	0.020
2.6	0.188	0.083	0.037
3.2	0.174	0.103	0.041
4.0	0.132	0.075	–
4.5	0.079	0.057	0.031
7.6	0.031	0.034	0.025
10.0	0.016	0.024	0.015
11.5	0.010	0.017	–
13.0	0.008	–	0.014

Table 2
Approximate values of charge carriers mobility for p-PbSe sample, estimated from transverse ($\mu_{TNE}(\Delta y/\Delta x)$) and longitudinal ($\mu_{LNE}$) Nernst–Ettingshausen effects at $T = 295$ K

P (GPa)	μ (m^2/V s)	
	$\mu_{TNE}(\Delta y/\Delta x)$	μ_{LNE}
0.7	0.002	–
1.1	0.004	–
1.5	0.007	0.021
2.4	0.068	0.048
3.7	0.054	0.039
5.1	0.023	0.031
6.9	0.022	0.029
8.4	0.026	–

is indirect, and relation $m \sim E_g$ valid for direct gap semiconductors was not realised [18,19].

According to the theoretical model [24,25] NaCl structure with metallic conductivity ought to be unstable for PbX crystals due to Peierls distortion, which doubles the lattice constant and lowers the system energy by the opening of semiconductor gap at Fermi level. From the results of present work it follows that at PbTe and PbSe, the gapless state (metallic character of electron bands) realised near $P \sim 3$ GPa (Figs. 4 and 5), that preceded the structural transformations really. High pressure GeS-type phases of PbX indeed have an orthorhombic structure with two-fold enlarged lattice parameter when compared with initial NaCl-phase [9].

4. Conclusion

The novel results obtained for PbX compounds showed that TM measurements at ultrahigh pressure are capable of clarifying the parameters of charge carriers (mobility, scattering mechanism) and hence, the type of electron structure of initial and high pressure phases even for complicated cases of semiconductors with more than one kind of charge carriers.

Decrease of temperature ought to increase significantly TM effects, as electron and hole mobilities in PbX are known to strongly enlarge [9]. In comparison with usual thermoelectric method of cooling based on Peltier effect the TM effects seem more perspective ones [26]. So, the technique developed of thermomagnetic measurements under pressure may have useful practical applications [27].

Acknowledgements

This work was partly supported by the Russian Foundation for Basic Research, Gr. No. 01-02-17203

References

[1] W. Paul, D. Warshawer, Solids Under Pressure, McGraw-Hill, 1963.
[2] W. Paul, J. Appl. Phys. 32 (1961) 2082.
[3] J.R. Patterson, S.A. Catledge, Y.K. Vohra, et al., Phys. Rev. Lett. 85 (2000) 5364.
[4] I.M. Tsidil'kovskii, V.V. Shchennikov, N.G. Gluzman, Fizika i Technika Poluprovodnikov 17 (1983) 958.
[5] V.V. Shchennikov, Fizika Tverdogo Tela 35 (1993) 401.
[6] I.M. Tsidil'kovskii, Thermomagnetic phenomena in semiconductors, State Publ. Phys.-Math. Lit., Moscow (1960).
[7] M.M. Aksel'rod, K.M. Demchuk, I.M. Tsidil'kovskii, Phys. Stat. Solid 27 (1968) 249.
[8] V.V. Shchennikov, S.V. Ovsyannikov, Solid State Commun. 121 (2002) 323.
[9] Yu.I. Ravich, B.A. Efimov, I.A. Smirnov, Methods of Semiconductor Investigation in Application to Lead Chalcogenides, Nauka, Moscow, 1968.
[10] G.A. Samara, H.G. Drickamer, J. Chem. Phys. 37 (1962) 1159.
[11] A.A. Semerchan, N.N. Kuzin, L.N. Drozdova, et al., Doklady Academii Nauk USSR, Physics 152 (1963) 1079.
[12] T. Chattopadhyay, H.G. Von Schnering, W.A. Grosshans, W.A. Holzapfel, Physica, BC 139–140 (1986) 356.
[13] S. Ves, Yu.A. Pusep, K. Syassen, M. Cardona, Solid State Commun. 70 (1989) 257.
[14] N.B. Brandt, D.V. Gitsu, N.S. Popovich, et al., Pis'ma v ZHETF 22 (1975) 225.
[15] V.V. Shchennikov, S.V. Ovsyannikov, A.Yu. Derevskov, Phys. Solid State 44 (2002) 1845.
[16] V.V. Shchennikov, A.V. Bazhenov, Rev. High Pressure Sci. Tech. 6 (1997) 657.
[17] V.V. Shchennikov, A.Yu. Derevskov, V.A. Smirnov, High Pressure Chemical Engineering, Elsevier, Amsterdam/Tokyo, 1996, pp. 667.
[18] B.M. Askerov, Kinetic Effects in Semiconductors, Nauka, St Petersburg, 1970.

[19] K. Seeger, Semiconductor Physics, Springer, Wien, NY, 1973.
[20] A.A. Averkin, S. Kasimov, E.D. Nensberg, Fizika Tverdogo Tela 4 (1962) 3669.
[21] A.A. Averkin, B.Y. Moyzhes, I.A. Smirnov, Fizika Tverdogo Tela 3 (1961) 1859.
[22] E.S. Itskevich, L.M. Kashirskaya, I.V. Kucherenko, et al., Pis'ma v ZHETF 43 (1986) 303.
[23] N.B. Brandt, O.N. Belousova, V.P. Zlomanov, et al., Fiz. Tverd. Tela 19 (1977) 437.
[24] B.A. Volkov, O.A. Pankratov, A.V. Sazonov, ZHETF 85 (1983) 1395.
[25] B.A. Volkov, O.A. Pankratov, S.V. Pakhomov, ZHETF 86 (1984) 2293.
[26] G.A. Ivanov, E.K. Iordanishvili, V.L. Naletov, et al., in: D.V. Gitsu, et al. (Eds.), Low Temperature Thermoelectric Materials, AN MSSR, Kishinev, 1970.
[27] S.V. Ovsyannikov, V.V. Shchennikov, Physica E17C (2003) 546.